Quantum Chemical Investigation of Thermal Cis-to-Trans Isomerization of Azobenzene Derivatives: Substituent Effects, Solvent Effects, and Comparison to Experimental Data

ARTICLE *in* THE JOURNAL OF PHYSICAL CHEMISTRY A · JUNE 2009

Impact Factor: 2.69 · DOI: 10.1021/jp9021344 · Source: PubMed

7 AUTHORS, INCLUDING:

Jonas Andre Wirth
Universität Potsdam
8 PUBLICATIONS **82** CITATIONS
SEE PROFILE

Stefan Hecht
Humboldt-Universität zu Berlin
186 PUBLICATIONS **5,772** CITATIONS
SEE PROFILE

Peter Saalfrank
Universität Potsdam
134 PUBLICATIONS **2,107** CITATIONS
SEE PROFILE

Quantum Chemical Investigation of Thermal Cis-to-Trans Isomerization of Azobenzene Derivatives: Substituent Effects, Solvent Effects, and Comparison to Experimental Data

Jadranka Dokić,[†] Marcel Gothe,[†] Jonas Wirth,[†] Maike V. Peters,[‡] Jutta Schwarz,[‡] Stefan Hecht,*[,‡] and Peter Saalfrank*[,†]

Institut für Chemie, Universität Potsdam, Karl-Liebknecht-Strasse 24-25, D-14476 Potsdam, Germany, and Institut für Chemie, Humboldt-Universität zu Berlin, Brook-Taylor-Strasse 2, 12489 Berlin, Germany

Received: March 10, 2009; Revised Manuscript Received: April 27, 2009

Quantum chemical calculations of various azobenzene (AB) derivatives have been carried out with the goal to describe the energetics and kinetics of their thermal cis → trans isomerization. The effects of substituents, in particular their type, number, and positioning, on activation energies have been systematically studied with the ultimate goal to tailor the switching process. Trends observed for mono- and disubstituted species are discussed. A polarizable continuum model is used to study, in an approximate fashion, the cis → trans isomerization of azobenzenes in solution. The nature of the transition state(s) and its dependence on substituents and the environment is discussed. In particular for push−pull azobenzenes, the reaction mechanism is found to change from inversion in nonpolar solvents to rotation in polar solvents. Concerning kinetics, calculations based on the Eyring transition state theory give usually reliable activation energies and enthalpies when compared to experimentally determined values. Also, trends in the resulting rate constants are correct. Other computed properties such as activation entropies and thus preexponential rate factors are in only moderate agreement with experiment.

I. Introduction

Molecular switches continue to attract attention lately in particular because of their potential use in nanotechnology ranging from information storage and processing to adaptive surfaces.[1−3] Azobenzenes (AB) are especially interesting because they can be switched from a trans to a cis isomer and vice versa by external stimuli (light, electrons, temperature). This is accompanied by a large geometrical transformation from the extended, flat trans form to the more three-dimensional and compact cis isomer. The structural change is associated with substantial alteration of the optical and electronic properties.

However, in order to exploit these features in nanotechnology, it is mandatory to arrange and interface the switch by attaching it to a solid surface. In fact, the switching of adsorbed azobenzenes enforced by light or the tip of a scanning tunneling microscope (STM), with either tunneling electrons or the electric field, has been successful.[4−9] In these examples metal surfaces were used and at least the light-induced switching[5,7−9] was found to occur only if the interaction between the azobenzene and the substrate was not too strong. This can be achieved by using bulky AB derivatives such as 3,3′,5,5′-tetra-*tert*-butyl-AB, called TBA in the following, whose extended *tert*-butyl "legs" decouple the molecule efficiently from the substrate. For orientation, the labeling of atoms used here and in the following is indicated in Figure 1.

As a concrete example, in refs 8 and 9 it was shown that TBA on Au(111) can be photoisomerized from trans to cis. In ref 9 the backreaction cis → trans was achieved only thermally so far. It was further demonstrated that for the thermal reaction rates and activation energies are very different from those

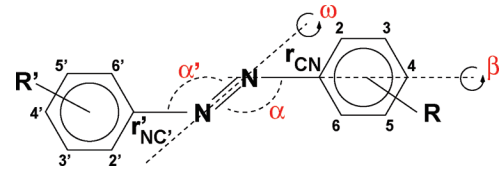

Figure 1. Labeling of atoms, and coordinates of the AB derivatives considered in this work.

obtained in solution.[8] In particular, the activation energy of the backreaction is much lower for the surface-confined species. Before the complicated details of thermal isomerization of azobenzenes on (metal) surfaces can be addressed, it is necessary to better understand the isomerization of free azobenzenes and of azobenzenes in a polarizable environment such as a solvent.

The thermal isomerization in solution has been known and/or predicted for azobenzene derivatives other than TBA for quite some time.[10−15] For a comprehensive review, the reader is referred to the work of Fanghänel et al.,[16] and references cited therein. In particular the dependence of the switching kinetics on the type, number, and positioning of substituents has been investigated experimentally. However, concerning the thermal cis → trans isomerization there is not much known from the theory side. From calculations (see below) it is known that the cis isomer is characterized by an inversion angle α (the N−N−C angle, see Figure 1) of about 120°, and a rotation angle ω (the dihedral angle C−N−N-C describing a rotation around the central N−N bond) of about 10°. The trans form has $\alpha \approx 120°$ and $\omega = 180°$. The cis → trans isomerization can, in principle, proceed along different reaction pathways and through various transition states. For example, on the basis of experiments it was speculated that the reaction might proceed by rotation around ω (without much change in α), with a transition state around $\omega \approx 90°$ and a formally broken N−N double bond. In most cases an energetically more favorable reaction path is the

* Corresponding authors, petsaal@rz.uni-potsdam.de and sh@chemie.hu-berlin.de.
[†] Institut für Chemie, Universität Potsdam.
[‡] Institut für Chemie, Humboldt-Universität zu Berlin.

10.1021/jp9021344 CCC: $40.75
Published on Web 05/19/2009

inversion along α with a linear transition state α ≈ 180° and an intact N−N double bond. For push−pull azobenzenes with a donor and an acceptor, a dipolar transition state (with some N−N single-bond character) was discussed.[17] In this case, depending on the solvent polarity, either inversion or rotation pathways may be operative. In general, the nature of the reaction depends on substituents, solvents, and pressure.[17]

From the theory side, quantum chemical calculations suggest that for certain azobenzenes the reaction is neither pure rotation around ω nor pure inversion along α, but a concerted motion along both degrees of freedom instead. For example, some calculations indicate a transition state with $\omega \approx 90°$ and $\alpha \approx 180°$.[18] Similarly, a transition state with a linear C−CH═N unit has been proposed for the related thermal imine isomerization long ago.[19] Regarding the question of how substituents and/or different solvents influence the thermal isomerization kinetics, it was suggested that for azobenzenes the isomerization rate can be accelerated by substituents in para position of the phenyl ring(s), irrespective of the substituent type.[20] As a consequence, one obtains a V-shaped Hammett plot.[20,21] Substituents were further found to have an additive effect on the kinetics when positioned at the same ring.[20] For azobenzenes substituted on different rings, the additivity rule does not hold according to experiment. Solvents with increasing dielectric constant increase the isomerization rate, and so does pressure,[17,22] at least in the case of push−pull azobenzenes. This supports the idea of a dipolar transition state in this case.

The goal of the present paper is to contribute to a better understanding of the thermal cis → trans isomerization kinetics of azobenzenes, and their dependence on substitution and solvent effects, from both a theoretical and an experimental point of view. The ultimate goal is the fine-tuning of the switching behavior of azobenzenes. Note that surface effects are not considered at the moment. However, among others, molecules with bulky substituents are being considered that have proven or may prove successful as surface-attached molecular switches. In the following, we are employing quantum chemical calculations. Some of the computational results for the bulky azobenzenes are being compared to experimental data.

The paper is organized as follows. In section II, the theoretical methods will be described. In most examples gas-phase calculations were carried out. To estimate solvent effects, the so-called polarizable continuum model (PCM) was used. In section III we present results for isomerization of azobenzenes in the electronic ground state. The nature of the transition state is discussed in section IIIA, and the influence of substituents in section IIIB. As substituents, (π-) donors and acceptors, but also electronically inactive (bulky) groups and push−pull azobenzenes with donors and acceptors, are studied also. In section IIIC we consider the kinetics of switching, by computing the thermal rates of isomerization and their temperature dependence. A comparison to experimental data is made for molecules studied also experimentally in this work, i.e., bulky azobenzenes as candidates for molecular switches at surfaces. In particular, five azobenzene derivatives with *tert*-butyl groups and other substituents were synthesized and spectroscopically analyzed and the kinetic parameters isomerization in solution was determined. Details of the synthesis and characterization are described in the Supporting Information. A final section, IV, concludes this work.

II. Computational Methodology

In this paper, we report quantum chemical calculations on AB derivatives using density functional theory using the B3LYP hybrid functional[23] and, if not otherwise specified, a 6-31G* basis set.[24−26] The Gaussian 03 program package[27] was used.

More than 90 AB derivatives were studied theoretically in this work. Among them are the parent azobenzene (AB) molecule, and TBA (3,3′,5,5′-tetra-*tert*-butyl-AB) as a prototype of bulky azobenzenes. Starting from AB, *monosubstituted* species with various substituents acting as donors via a resonance-mediated +M effect (−OMe, $-NH_2$), or as acceptors via a −M effect (−CN, $-NO_2$) were investigated theoretically. The substituents were placed in different positions, e.g., in para and meta positions. The models were then extended to disubstituted species, with two substituents of the same type ($-NH_2$, −OMe, −CN or $-NO_2$) at the same or at two different phenyl rings. An example for the former is 2,4-dicyano-AB, an example for the latter is 2,4′-dicyano-AB. We also considered several push−pull azobenzenes with a donor (e.g., $-NH_2$) on one ring and an acceptor (e.g., $-NO_2$) on the other, e.g., 4-NO_2−4′-NH_2-AB, also called Disperse Orange 3 (DO3). A few triply substituted azobenzenes, such as 2,4,6-tricyano-AB, were also studied.

For direct comparison to experimental data for species investigated as switches adsorbed at noble metals surfaces, mono- and disubstituted species were constructed starting from TBA,[28,29] by adding substituents in para positions: 4-methoxy-TBA (M-TBA for short) and 4,4′-dimethoxy-TBA (diM-TBA).[30] Further, derivatives were considered in which two *tert*-butyl groups of TBA were replaced by −COOH groups, i.e., 3,5-di-*tert*-butyl-3,5′-dicarboxyl-AB (DBDCA),[31] or in which two of the four *tert*-butyl groups were rearranged, 2,2′,5,5′-tetra-*tert*-butyl-AB (TBA′)—see the Supporting Information for details.

For all of these molecules, treated as gas phase species, we determined the minima corresponding to cis and trans isomers by geometry optimization. Transition states for the cis ↔ trans reaction were obtained by the synchronous transit-guided quasi-Newton method (QST2 and QST3).[32−34] Normal mode analysis of the transition structures delivered a single imaginary frequency. For selected cases, also full two-dimensional potential energy surfaces $V(\alpha,\omega)$ were computed by selecting an (α,ω) pair and reoptimizing all other geometry parameters. This allows one to estimate the importance and energetics of alternative reaction pathways.

As an example of the transition state search Figure 2 depicts the optimized minimum structures of cis and trans configurations of TBA as well as the corresponding transition state. The latter is linear with respect to the NNC moiety ($\alpha \approx 180°$) and has one phenyl ring rotated relative to the other ($\omega \approx 90°$). Note that for exact $\alpha = 180°$, ω is not strictly defined. This indicates that motions along both α and ω are necessary to reach the transition state.

Once stationary points (minima, transition states) were identified, frequency analyses at these points provide thermochemical properties. For example, the Gibbs free

$$G = H - TS \tag{1}$$

is calculated with an enthalpy H given under ideal gas conditions, as

$$H = U_{el} + U_{vib} + U_{rot} + U_{trans} + pV \tag{2}$$

$$H = E_{el} + E_{ZPE} + \Delta E_{vib}(T) + 4RT \tag{3}$$

Here $U_{el} = E_{el}$ the electronic energy calculated from B3LYP, $U_{vib} = E_{ZPE} + \Delta E_{vib}(T)$ the zero-point (E_{ZPE}) and thermal (ΔE_{vib})

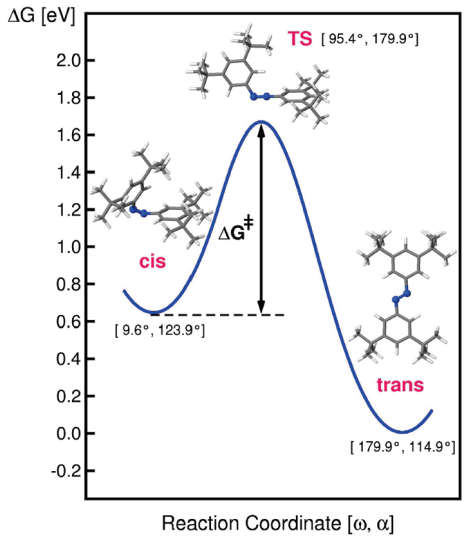

Figure 2. Schematics of the thermal isomerization of the TBA molecule from cis to trans along a "reaction coordinate" via a transition state. Geometries with computed α and ω angles and changes of the Gibbs free energy, relative to the cis form, are shown. The calculations were done on the B3LYP/6-31G* level of theory.

vibrational contribution to the energy, and $U_{rot} = (3/2)RT$, $U_{trans} = (3/2)RT$ are the rotational and translational contributions to U. We have further $pV = RT$ for an ideal gas, $E_{ZPE} = L\sum_i(1/2)h\nu_i$ (i labels the vibrational normal modes with frequencies ν_i, L is Avogradro's constant), $\Delta E_{vib}(T) = L\sum_i h\nu_i (\exp(h\nu_i/k_BT) - 1)^{-1}$. One can also calculate the heat capacity at constant volume V

$$C_V = \left(\frac{\partial U}{\partial T}\right)_V = 3R + \frac{\partial \Delta E_{vib}(T)}{\partial T} \quad (4)$$

which is temperature dependent. Neglecting the (weak) temperature dependence by setting $C_V = C_V(T_0)$, where T_0 is a suitable "reference temperature", the temperature dependence of U is simply $U(T) = U(0) + C_V(T_0)T$. Here, $U(0) = H(0) = E_{el} + E_{ZPE}$ is the energy (enthalpy) at $T = 0$. Neglecting further the (also weak) T-dependence of the entropy S in eq 1, we can approximate the *activation free energy* $\Delta G^{\ddagger}$ as

$$\Delta G^{\ddagger}(T) = \Delta H^{\ddagger}(0) + \Delta C_V^{\ddagger}(T_0)T - \Delta S^{\ddagger}(T_0)T \quad (5)$$

Here, $\Delta B^{\ddagger} = B^{\ddagger} - B(R)$ is a general symbol for a property ($B = H$, ΔC_v, S, or G) of the transition state (‡) or the reactant (R), i.e., the cis isomer in the case of cis → trans isomerization. Equation 5 has the advantage of giving $\Delta G^{\ddagger}$ for all T without the need to recalculate the thermodynamic properties at every temperature. As the reference temperature $T_0 = 298.15$ K (room temperature) was chosen. The approximation (5) to calculate $\Delta G^{\ddagger}(T)$ has been checked and found to be a very good one. For the specific example of TBA at room temperature, the procedure is illustrated in Figure 2.

From $\Delta G^{\ddagger}$, the isomerization rate $k_{c\to t}$ is calculated as a function of temperature according to Eyring transition state theory[35]

$$k_{c\to t}(T) = \frac{k_BT}{h} e^{-\Delta G^{\ddagger}/RT} \quad (6)$$

$$k_{c\to t}(T) = \frac{k_BT}{h} e^{-\Delta C_V^{\ddagger}/R} e^{\Delta S^{\ddagger}/R} e^{-\Delta H^{\ddagger}(0)/RT} \quad (7)$$

In several cases we plot $\ln(k_{c\to t})$ vs $1/T$ and get an almost perfect linear curve. From a linear fit, an "effective" activation energy E_a can then be obtained from the slope and an effective prefactor A from the intercept of the curve in the case we are interested in the parameters of a simple Arrhenius form

$$k_{c\to t}(T) = Ae^{-E_a/RT} \quad (8)$$

The notion "effective" refers to the fact that the Arrhenius parameters are not precise. Solvent effects are included in an approximate way only. For this purpose we use the *polarizable continuum model* (PCM), first proposed by Tomasi and coworkers.[36] That is, the molecules under investigation are embedded in a polarizable continuum, characterized by a dielectric constant ε. Another solvent-specific parameter of the PCM is the size of a solvent molecule. As a continuum model the PCM does not account for the detailed effects of the solvent on a molecular level. In particular it does not account for the rearrangement of solvent molecules during the formation of the transition state. The correct calculation of free energy surfaces and rates for molecules in solution would also require the explicit inclusion of the thermal motion of solvent molecules.[37] The PCM model does, however, account for the stabilization/destabilization of stationary structures due to polarization. In the approach used here, the stationary points are recalculated in the PCM field and so are the vibrational frequencies to obtain thermochemical data. For TBA, cyclohexane was sometimes assumed as the solvent to relate to the experiments described in the Supporting Information. For the push−pull azobenzene DO3, several solvents with a wide range of dielectric constants were modeled within the PCM scheme.

III. Results and Discussion

A. Nature of the Transition State. As already indicated in Figure 2, the transition state suggests that along the lowest-energy path connecting the cis and trans isomers both α and ω change, giving rise to an (almost) linear N−N−C moiety ($\alpha \approx 180°$), and one phenyl ring rotated relative to the other ($\omega \approx 90°$). For TBA, one finds that the reaction energy $\Delta E_{ct} = E_{el}(\text{trans}) - E_{el}(\text{cis}) = 0.65$ eV. The activation enthalpy at $T = 0$ for cis → trans isomerization, i.e., the zero-point corrected energy barrier, is $\Delta H^{\ddagger}(0) = 1.18$ eV. The ZPE correction is 0.07 eV; i.e., the classical barrier is $\Delta E_{el}^{\ddagger} = 1.11$ eV.

The observation that the transition state requires the simultaneous change of α and ω is also supported by the potential energy surface (PES) $V(\alpha,\omega)$. $V(\alpha,\omega)$ was calculated for azobenzene itself and for azobenzenes with electronically only weakly active substituents such as 4-adamantyl-AB. Both AB and 4-adamantyl-AB behave very similar to TBA, with classical activation energies $\Delta E_{el}^{\ddagger}$ of 1.10 eV (for AB) and 1.11 eV (for 4-adamantyl-AB), and reaction energies ΔE_{ct} of 0.66 eV for both. During the potential surface scan all degrees of freedom other than ω and α were not constrained and reoptimized at each step. The dihedral and inversion angles ω and α were scanned with intervals of 10° steps, starting from the geometry of the cis isomer. From $V(\alpha,\omega)$, which is similar to the findings reported earlier[38] and which is not shown for brevity here, one obtains the following information:

(1) When isomerizing directly from cis to trans configuration along a pure inversion path by only changing α (not ω), the

TABLE 1: Selected Geometry Parameters of AB, TBA, and 4-Adamantyl-AB in the Cis Configuration and at the Transition State for Cis → Trans Isomerization[a]

molecule	ω	α	α'	r_{NN}	r_{CN}	$r'_{C'N}$	$\Delta E_{el}^{\ddagger}$	ΔE_{ct}
AB (cis)	9.8	124.1	124.1	1.250	1.436	1.436		
AB‡	90.0	179.4	117.0	1.226	1.335	1.453	1.10	0.66
TBA (cis)	9.5	124.1	124.1	1.261	1.437	1.437		
TBA‡	87.7	179.9	117.1	1.227	1.336	1.453	1.11	0.65
4-adamantyl-AB (cis)	10.0	124.1	124.1	1.250	1.436	1.436		
4-adamantyl-AB‡	90.0	179.1	117.2	1.227	1.334	1.448	1.11	0.66

[a] All angles are given in degrees, all distances in angstroms. The last two columns give the classical barrier for cis → trans isomerization, $\Delta E_{el}^{\ddagger}$, and the reaction energy ΔE_{ct} in electronvolts.

TABLE 2: Activation Parameters and Kinetics of Isolated, Mono-substituted Azobenzenes, Computed at the B3LYP/6-31G* Level of Theory[a]

molecule	$\Delta E_{el}^{\ddagger}$	$\Delta H(0)^{\ddagger}$	$\Delta S^{\ddagger}$	ΔC_V	$\Delta G^{\ddagger}(298.15)$	$k_{c\rightarrow t}(298.15)$	A	E_a	σ
AB	1.10	1.17	+13.91	−1.15	1.11	8.19×10^{-5}	2.33×10^{13}	1.17	0.00
4-CN-AB	0.91	0.97	+4.22	−1.98	0.95	2.52×10^{-2}	7.93×10^{12}	0.97	+0.86
4-NO_2-AB	0.83	0.89	−0.64	−2.34	0.88	2.70×10^{-1}	4.57×10^{12}	0.89	+1.25
4-ada.-AB	1.11	1.15	+14.21	−0.78	0.98	1.39×10^{-4}	3.46×10^{13}	1.03	--
4-OMe-AB	1.07	1.14	+5.78	−1.22	1.11	8.52×10^{-5}	8.84×10^{12}	1.14	−0.27
4-NH_2-AB	1.03	1.04	+7.86	−0.91	1.06	5.05×10^{-4}	1.09×10^{13}	1.09	−0.66
3-CN-AB	1.02	1.09	+6.08	−1.52	1.06	5.26×10^{-4}	7.93×10^{12}	1.09	0.56
5-NO_2-AB	1.01	1.08	+6.13	−1.60	1.05	7.54×10^{-4}	9.57×10^{12}	1.08	+0.71
5-NH_2-AB	1.08	1.14	+8.29	−1.23	1.11	9.71×10^{-5}	1.19×10^{13}	1.14	−0.16

[a] Energies in electronvolts, entropies and heat capacities in J/(K mol), rates and prefactors in s^{-1}. The last column gives Hammett substituent constants σ, taken from ref 39. Some of the σ values of ref 39 are different from the original Hammett values and have been especially adapted for azobenzenes.

activation energy itself remains almost unaffected. In general, the 2D PES supports several "inversion" pathways which go through maxima of similar height,[38] but in most cases not a minimum-energy path is followed or the local maxima are not proper transition states.

(2) When isomerizing from cis to trans configuration by pure rotation, i.e. changing ω at fixed $\alpha = \alpha_{cis}$, one goes through a maximum at $\omega \approx 90°$, which is close to a conical intersection and corresponds to an activation energy of about 1.4 eV.

For most of the ABs studied here, linear or almost linear transition states with $\alpha \approx 180°$ were found. In the case of unsymmetrically substituted species two different TS with linear α or α' (see Figure 1) are possible—see below. Further on it will also be shown that for push−pull AB a rotation pathway without a linear transition state is possible, depending on the polarity of the solvent. Even in the majority of cases where a linear TS with α (α') $\approx 90°$ is found, ω is also rotated, to $\omega \approx 90°$. Geometry parameters other than α and ω are generally not so much affected in the TS. For AB, TBA, and 4-adamantyl-AB, for example, the biggest change is found for the length of the N−C bond involved in isomerization, which is shortened by about 0.1 Å in the TS due to some C−N double bond character. Other bond lengths hardly change relative to the cis (and trans) configurations, as demonstrated in Table 1.

B. Activation Energies: Substituted Azobenzenes. ***1. Electronically "Inactive" Species.*** The results summarized in Table 1 support the finding mentioned above that substitution of H by alkyl groups (*tert*-butyl or adamantyl) does not change the properties and thermal switching behavior (i.e., the activation energy) significantly. This can be expected since alkyl substitution has mainly steric effects while the conjugated π-system remains unaffected.

2. Monosubstitution with Electronically "Active" Species. The situation is different for azobenzenes with substituents showing mesomeric effects. This is demonstrated in Table 2, which lists properties of azobenzenes in which a H atom has been replaced by either −CN or −NO_2 (both with a −M effect) or −NH_2 or −OMe (both with a +M effect). Pure azobenzene and 4-adamantyl-AB are shown for comparison.

In the table, four different types of "activation energies" are shown, namely, the classical barrier $\Delta E_{el}^{\ddagger}$, the zero-point corrected barrier at $T = 0$, $\Delta H(0)^{\ddagger} = \Delta E_{el}^{\ddagger} + \Delta E_{ZPE}^{\ddagger}$, the Gibbs free activation energy at room temperature, $\Delta G(298.15)^{\ddagger}$ from eq 5, and finally the Arrhenius activation energy, E_a, obtained from a linear fit of $\ln(k_{c\rightarrow t})$ vs $1/T$ and employing the Arrhenius expression (8). Comparing these four energies, we note that, similar to TBA, the zero-point corrections are in most cases around 0.07 eV (with the exception of 4-NH_2-AB, where it is smaller), and they increase the classical barrier. The thermal correction to the enthalpy and the entropy contribution are usually slightly smaller than zero-point corrections, between 0.01 and 0.06 eV according to Table 2, tending to lower the barrier. Finally, the fitted activation energy, E_a, is in most cases almost identical to the zero-point corrected barrier at $T = 0$.

Concerning the trends enforced by substituents, the following is observed.

(1) Substituents in para position (4) reduce the barrier(s). In particular, substituents with a −M effect (−CN, −NO_2) are efficient, lowering the barrier by up to about 0.3 eV for the strongest acceptor, −NO_2. The substituents with a +M effect (−OMe, −NH_2) or no M effect (−adamantyl) are much less efficient and have barriers similar to those of AB. The lower barrier for π-acceptors can easily be explained with simple mesomeric formulas, which indicate that a linear transition state can be stabilized by an acceptor in the para position, as indicated in Figure 3. The figure shows that also an acceptor in the ortho position stabilizes the linear transition state. It will be shown below that an acceptor in the ortho position is as efficient as one in the para position. On the other hand, if a donor is in a para or ortho position, no large stabilization is expected since the corresponding resonance structures are unlikely. This explains the only slightly reduced barriers (less than 0.1 eV), and slightly altered rates (by less than a factor of 10), relative to AB according to Table. 2.

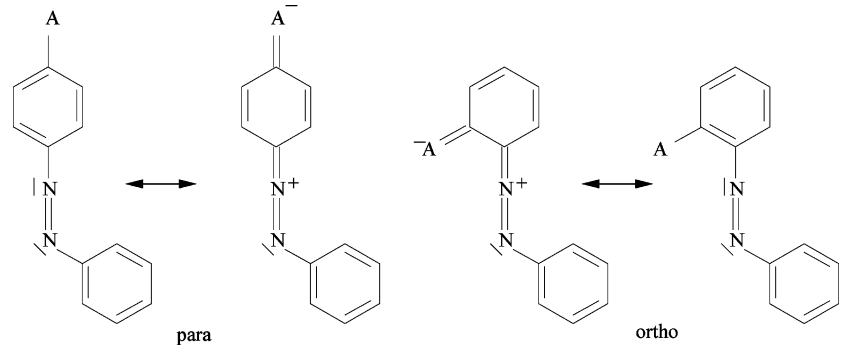

Figure 3. Mesomeric structures of an azobenzene with a linear N−N−C unit and an acceptor in a para or in ortho position.

TABLE 3: Energetics of Diaminoazobenzenes, All Energies in eV: Left, Disubstitution on One Ring; Right, Disubstitution on Two Rings

type	substituents	ΔE_{ct}	$\Delta E_{el}^{\ddagger}$	substituents	ΔE_{ct}	$\Delta E_{el}^{\ddagger}$
o,o				3,2′-NH_2	0.60	1.22
o,m	2,3-NH_2	0.70	1.05	2,3′-NH_2	0.61	1.11
o,p	2,4-NH_2	0.64	1.06	2,4′-NH_2	0.67	1.21
o,m	2,5-NH_2	0.64	1.02	2,5′-NH_2	0.62	1.11
o,o	2,6-NH_2	0.90	0.90	2,6′-NH_2	0.79	1.16
m,m				3,3′-NH_2	0.63	1.13
m,p	3,4-NH_2	0.70	1.05	3,4′-NH_2	0.67	1.08
m,m	3,5-NH_2	0.64	1.15	3,5′-NH_2	0.64	1.11
m,o	3,6-NH_2	0.85	1.07	3,6′-NH_2	0.89	0.98
p,p				4,4′-NH_2	0.74	1.18
p,m	4,5-NH_2	0.70	1.05	4,5′-NH_2	0.69	1.22
p,o	4,6-NH_2	0.78	1.02	4,6′-NH_2	0.90	1.17
m,m				5,5′-NH_2	0.66	1.24
m,o	5,6-NH_2	0.74	1.05	5,6′-NH_2	0.89	0.99
o,o				6,6′-NH_2	1.07	1.02

(2) Similarly, also for donors or acceptors in the meta position (3 or 5), no stabilizing effect is expected from the mesomeric structures. Also here only small changes of barriers and moderate enhancement of rate constants are observed according to Table 2, lower half.

Of course, arguments based on resonance structures are simplified. A step further is analysis at the molecular orbital level, which gives the same result: Acceptors stabilize the HOMO of the TS when in para (or ortho) positions, while donors have a negligible effect. Further, the frontier orbitals have nodes in the meta positions, consistent with the observation that both donors or acceptors in this position make a small effect only. In summary, substitution appears to be beneficial in most cases. The amount of barrier reduction depends, however, strongly on type and position of the substituents. Barrier reduction will result in accelerated reactions. That para substitution accelarates the cis → trans isomerization irrespective of the type of substituent is known for a long time.[20] Kinetics will be discussed more extensively below in section IIIC.

In passing we note that, in agreement with earlier observations,[15,20] we also find that azobenzenes isomerize through inversion of the N-atom adjacent the substituted side in the case of acceptors substitution but on the N-atom adjacent to the nonsubstituted aryl moiety in the case of donor substitution. In other words, an acceptor in positions 2−6 of Figure 1 leads to $\alpha \approx 180°$ in the TS, while a donor in positions 2−6 leads to $\alpha' \approx 180°$ instead.

3. Double Substitution with Donors. Subsequently double-substitution was studied, first with donors. As donors of the +M type the amino $-NH_2$ and methoxy groups −OMe were again chosen. Disubstitution took place either on a single benzene ring or on both. In Table 3 we show the cis → trans activation energies $\Delta E_{el}^{\ddagger}$, and the cis → trans reaction energy, ΔE_{ct} for a number of selected diaminoazobenzenes.

From the Table, the following conclusions can be drawn:

(1) If substituents are on one ring (left half of the table), the classical inversion barriers $\Delta E_{el}^{\ddagger}$ depend only weakly on their position. The barriers vary between 0.9 and 1.15 eV. By far most values are only slightly lower than for AB (1.10 eV) and in the order of monosubstituted aminoazobenzenes. For comparison, for monoamines 4-NH_2-AB and 5-NH_2-AB the classical activation energies were 1.03 and 1.08 eV, respectively (see Table 2). The low activation energy for 2,6-NH_2-AB of $\Delta E_{el}^{\ddagger} = 0.9$ eV is an exception and due to the fact that the cis form is destabilized in this case. The relative insensitivity of the barrier to donor substitution is consistent with the same observation made for the related monosubstituted species.

(2) The energy differences ΔE_{ct} between cis and trans vary for disubstitution on one ring (left half) or on two rings (right half of the table), between 0.61 and 0.9 eV, with the exception of 6,6′-NH_2-AB with $\Delta E_{ct} = 1.07$ eV. Large values of ΔE_{ct} are associated with the steric destabilization of the compact cis form.

(3) For substitution on two rings (right half of Table 3), the cis → trans activation energies $\Delta E_{el}^{\ddagger}$ are between 0.98 and 1.24 eV for the cases shown. Thus, the activation energies can now be lower or higher when compared to AB (1.10 eV), in contrast to substitution on one ring only where it was lower for almost all examples. The lowest activation energies are found when ΔE_{ct} is large, which is the case for one or two substituents in the ortho position.

A strong dependence on the number and positioning of the substituents is observed for the dipole moment. For the diaminoazobenzenes the dipole moment varies between zero (in the case of *trans*-5,5′-NH_2-AB) to 6.64 D (for *cis*-4,5′-NH_2-

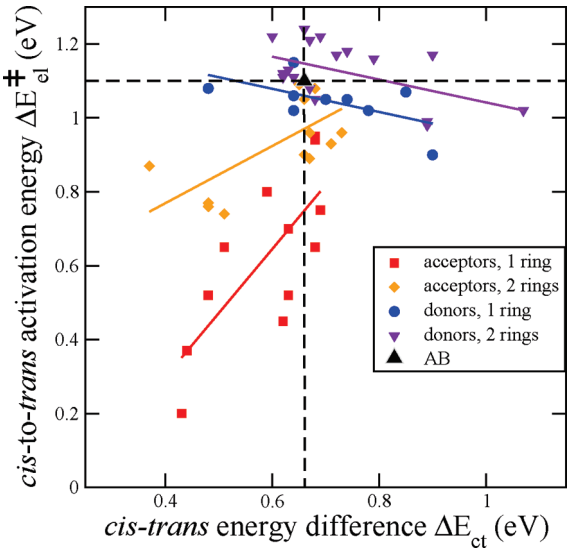

Figure 4. ΔE_{ct} vs $E_{el}^{\ddagger}$ plot for different classes of double- and triple-substituted azobenzenes: acceptors on one ring, acceptors on two rings, donors on one ring, and donors on two rings. The vertical and horizontal dashed lines indicate the values found for azobenzene, indicated as a big triangle oriented upward. Full lines serve as guides to the eye (obtained by linear regressions) for each of the four classes of substituted azobenzenes.

AB). For comparison, the dipole moment of *cis*-AB is 3.22 D on the B3LYP/6-31G* level of theory.

For dimethoxyazobenzenes we find qualitative trends very similar to those of diaminoazobenzenes. Altogether, 12 different dimethoxyazobenzenes were studied. The inversion barriers $\Delta E_{el}^{\ddagger}$ for cis → trans isomerization are between 1.05 eV (for 3,4′-OMe-AB) and 1.17 eV (for 4,4′-OMe-AB). Further, the cis−trans energy differences ΔE_{ct} are smaller than those of the diaminoazobenzenes: They range from 0.43 eV (for 2,6-OMe-AB) to 0.72 eV (for 4,4′-OMe-AB). The fact that ΔE_{ct} is so low for 2,6-OMe-AB in comparison to 2,6-NH_2-AB (0.90 eV) indicates that steric destabilization of ortho substituents plays no major role for the linear −OMe group.

As in the case of diaminoazobenzenes in dimethoxyazobenzenes there is a correlation between negative reaction energy and activation energy: $\Delta E_{el}^{\ddagger}$ tends to decrease with increasing negative reaction energy, $\Delta E_{ct} = E_c - E_t$. This indicates an approximate linear free energy relationship,[40] as supported by $\Delta E_{el}^{\ddagger}$ vs ΔE_{ct} plots in Figure 4. The figure shows that the slope of a linear regression to the data is about the same for donor substitution on either one or two rings, with the former, however, causing lower activation energies.

4. Double- and Triple-Substitution with Acceptors. As for single substitution, introduction of two acceptor groups, e.g., cyano (−CN) or nitro (−NO_2) groups leads to a linear transition state which can be stabilized by acceptors placed in para and ortho positions. This is demonstrated in Table 4 where 13 different dinitroazobenzenes and a single trinitroazobenzene are considered.

From the Table, the following conclusions can be drawn:

(1) Electron acceptors in ortho and para positions lower the cis → trans barriers significantly, in particular when they are located on the same phenyl ring (left half of the table). For example, the barrier for azobenzene of 1.10 eV reduces to 0.83 eV for 4-NO_2-AB, further to 0.52 eV for 2,4-NO_2-AB, and finally to 0.20 eV for 2,4,6-NO_2-AB. Thus every nitro group in the ortho or para position of one ring lowers the barrier by about 0.3 eV. In this case, ortho substitution is slightly more effective

TABLE 4: Energetics of Di- and Trinitroazobenzenes, All Energies in eV: Left, Substitution on One Ring; Right, Substitution on Two Rings

substituents	ΔE_{ct}	$\Delta E_{el}^{\ddagger}$	substituents	ΔE_{ct}	$\Delta E_{el}^{\ddagger}$
2,4-NO_2	0.48	0.52	2,2′-NO_2	0.37	0.87
2,5-NO_2	0.51	0.65	2,3′-NO_2	0.51	0.74
2,6-NO_2	0.44	0.37	2,4′-NO_2	0.48	0.77
3,5-NO_2	0.68	0.94	2,5′-NO_2	0.48	0.76
3,6-NO_2	0.63	0.52	3,3′-NO_2	0.70	1.05
2,4,6-NO_2	0.43	0.20	3,4′-NO_2	0.67	0.89
			4,4′-NO_2	0.65	1.09
			4,5′-NO_2	0.66	0.90

than para substitution, e.g., the barrier for 2,6-NO_2-AB (two ortho substituents) is 0.37 eV, while the barrier for 2,4-NO_2-AB (one ortho, one para substituent) is 0.52 eV.

An additivity rule for barriers naturally translates into an additivity rule for logarithmic rates. Assuming an additivity rule for activation energies implies $E_{el}^{\ddagger} \approx E_{el}^{\ddagger}(0) + \sum_i \Delta_i$ where $E_{el}^{\ddagger}(0)$ is the activation energy without substituents and Δ_i the barrier change due to substituent i. The latter is $\Delta_i \approx -0.3$ eV both for *o*- and *p*-NO_2. Assuming an Arrhenius law and setting $E_a \approx \Delta E_{el}^{\ddagger}$, we get

$$\ln k_{c\to t} = \ln k_0 - \sum_i \frac{\Delta_i}{RT} \qquad (9)$$

where k_0 is the isomerization rate constant for the unsubstituted species. Similar additivity rules have been observed experimentally.[20]

(2) Also the ortho and/or para substitution at two different phenyl rings lowers activation barriers considerably. Here, however, the additivity rule for activation energies does not hold: In 4,4′-NO_2-AB, for example, the activation energy is 1.09 eV and thus *higher* than that for a singly, para-substituted ring: $\Delta E_{el}^{\ddagger}$ (4-NO_2-AB) = 0.83 eV according to Table 1. The absence of a simple additivity rule for two-ring substitution is in agreement with experimental observations.[20] A simple explanation comes from the mesomeric structures shown in Figure 3: Only an acceptor on the ring, which is directly attached to the inverting N-atom stabilizes a linear transition state.

(3) Acceptors in meta positions (3, 3′, 5, 5′) are generally quite inefficient, as expected. For instance, the barrier of 4-NO_2-AB of 0.83 eV is only slightly altered if a NO_2 group is added in the meta position of the neighboring phenyl ring: $\Delta E_{el}^{\ddagger}$ (3,4′-NO_2-AB) = 0.89 eV.

(4) The activation energy $\Delta E_{el}^{\ddagger}$ correlates with the (negative) reaction energy ΔE_{ct}, indicating a linear free energy relationship as for donor substitution. In contrast to donor substitution, however, large ΔE_{ct} values are usually associated with lower activation energies.

The nitro groups affect the geometries of the stable molecules, cis and trans. The dihedral angle ω of cis isomers (which is around 10° for the AB), ranges now from 2.2° for 3,6-NO_2-AB up to 18° for 2,2′-NO_2-AB. Usually molecules with acceptors in meta positions have, because of steric hindrance, higher ω values. Bond lengths are only slightly affected. Dipole moments of disubstituted azobenzenes are sometimes quite high, both for cis and trans isomers. The highest dipole moment is found for *trans*-2,5′-NO_2-AB, with $|\mu| = 8.07$ D.

We also studied 14 different di- and trisubstituted cyanoazobenzenes. Also here, quite low barriers are observed. The lowest one was for 2,4,6-CN-AB, with $\Delta E_{el}^{\ddagger} = 0.45$ eV.

TABLE 5: Energetics of Push−Pull Azobenzenes, All Energies in eV: Left, 4,4′-Substitution; Right: Other Substitutions

substituents	ΔE_{ct}	$\Delta E_{el}^{\ddagger}$	substituents	ΔE_{ct}	$\Delta E_{el}^{\ddagger}$
4CN−4′OMe	0.69	0.87	$2NO_2$−2′NH_2	0.48	0.68
4CN−4′NH_2	0.69	0.85	$2NO_2$−3′NH_2	0.47	0.70
$4NO_2$−4′OMe	0.68	0.79	$2NO_2$−4′NH_2	0.53	0.63
$4NO_2$−4′NH_2	0.68	0.77	$3NO_2$−2′NH_2	0.63	1.01
			$3NO_2$−3′NH_2	0.64	1.01
			$3NO_2$−4′NH_2	0.71	0.94
			$4NO_2$−2′NH_2	0.61	0.84
			$4NO_2$−3′NH_2	0.62	0.83
			$4NO_2$−5′NH_2	0.65	0.83
			$4NO_2$−6′NH_2	0.97	0.68

Substitution on one ring leads to lower barriers than substitution on two rings. For instance, the classical activation energy is 0.96 eV for 2,2′-CN-AB (two ortho substituents on different rings) and only 0.70 eV for 2,6-CN-AB (two ortho substituents on the same ring). As expected, ortho and para substitution is much more efficient than meta substitution. For example, 2,4-CN-AB (o,p) has a barrier of 0.65 eV, and 3,5-CN-AB (m,m) a barrier of 0.95 eV. Again, for substitution on one ring the reduction of activation energies is approximately additive, with each para and/or ortho substituent lowering the barrier by about 0.2 eV: $\Delta E_{el}^{\ddagger} = 0.91$ eV, 0.65 eV, and 0.45 eV for 4-CN-AB, 2,4-CN-AB, and 2,4,6-CN-AB, respectively. In summary, −CN substitution shares many similarities with $-NO_2$ substitution. Quantitatively, the stronger acceptor $-NO_2$ has a bigger effect on lowering barriers. Another possible contribution comes from steric effects, which tend to lower the energy difference between the cis form and the TS, more so for the bulky $-NO_2$ than for linear −CN. Dipole moments are tentatively larger for the cyano compounds: The largest dipole moment was for 2,5′-CN-AB, $|\mu| = 8.49$ D.

The findings for azobenzenes with two or three acceptors are summarized in Figure 4. Again, approximate linear free energy relationships are found between activation and (negative) reaction energies. The slopes of linear regressions to the data are now large and positive, in contrast to donor substitution. Acceptor substitution on one ring leads to the lowest activation energies of all azobenzenes studied in this work.

Finally, a word about the nature of transition states. We observe that if two acceptors are at the same ring, e.g., in positions 2−6 of Figure 1, then linearization in the TS occurs at that ring (i.e., $\alpha \approx 180°$). If one acceptor is on one ring and a second one on the other, linearization occurs at the ring which carries the strongest acceptor ($-NO_2 > -CN$) and/or in which the electronically "most active position" is substituted (ortho ≈ para > meta). If two identical acceptors are at two equivalent positions, then there are two equivalent transition states. Similar observations can be made for donors. If two donors are at the same ring, e.g., in positions 2−6 of Figure 1, then linearization in the TS occurs at the other ring (i.e., $\alpha' \approx 180°$). With one donor on one and another donor at the other ring, it depends on the nature of the donor and its position.

5. Push−Pull Azobenzenes. Push−pull azobenzenes have been of interest for many years for various reasons. In particular it has been speculated that the isomerization mechanism changes from the inversion type in less polar solvents to a rotation pathway in very polar environments.[17]

In Table 5 (left) we compare classical activation energies $\Delta E_{el}^{\ddagger}$ and negative reaction energies ΔE_{ct}, for four different push−pull azobenzenes with either −CN or $-NO_2$ in para position (4) of ring 1, and −OMe or $-NH_2$ in para position (4′) of ring 2. The barriers are sligthly below 0.8 eV for the NO_2-based compounds, i.e., slightly below the value of single-substituted 4-NO_2-AB of 0.83 eV (see Table 2). Similarly, for the CN-based azobenzenes the barriers are slightly below 0.9 eV, similar to single-substituted 4-CN-AB with a barrier of 0.91 eV. Thus, as expected, a donor in 4′-position lowers the activation energy only slightly. The lowest barrier of all 4,4′-push−pull azobenzenes studied is for DO3 ($4NO_2$−4′NH_2-AB), with $\Delta E_{el}^{\ddagger} = 0.77$ eV. For all 4,4′-push−pull systems, the energy difference between their cis and trans forms is slightly below 0.7 eV, i.e., close to conventional azobenzenes.

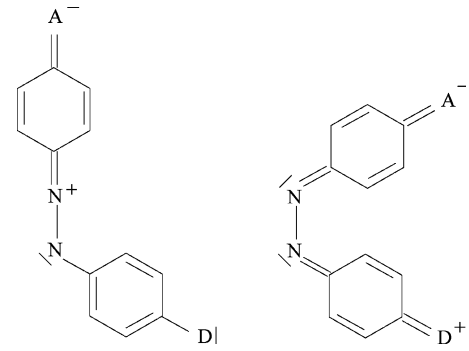

Figure 5. Mesomeric structures of push−pull azobenzenes participating to stabilize linear (left) or bent (right) TS associated with inversion and rotation, respectively.

On the right-hand side of the Table, compounds are listed with nitro groups in various (not necessarily para) positions, and amino groups in various positions on the other ring. The observed trends in activation energies are rationalized by the findings detailed above: A nitro group in the ortho position (2) lowers the barrier slightly more than the same group in the para position (4); a nitro group in the meta position (3) is largely inefficient, giving the highest barriers. The amino group has a small, barrier-lowering effect, which is largest if attached in the para (4′) position. Compounds with $-NO_2$ in the para position (4) and $-NH_2$ in the ortho (2′) or meta orientation (3′), have slightly higher barriers than DO3; however, the effect is small. In passing we note that an approximate linear free energy relationship is also found for push−pull azobenzenes, quantitatively similar to what was found in the case of double-substitution of acceptors on a single ring.

The dipole moments of push−pull azobenzenes are quite large, in particular for the 4,4′ species. The largest dipole moment is found for DO3, with $|\mu| = 9.79$ D for the trans isomer. In this case donor and acceptor are on opposite sides of the molecule at the largest possible distance. The dipole moment increases in polar solvents. For instance, in DMSO ($\varepsilon = 46.7$) we find $|\mu| = 15.46$ D when using a polarizable continuum model (see below).

In all of the gas phase examples of Table 5 the transition state was of the inversion-type, i.e., a NNC unit becomes (almost) linear. The left sketch in Figure 5 depicts a mesomeric structure, which stabilizes a linear transition state. This mesomeric structure is analogous to the one shown in Figure 3, on the left. Alternatively a mesomeric structure with a formal NN single bond can be envisioned (Figure 5, right), which is stabilized by its zwitterionic character. This mesomeric form would allow for a rotation mechanism with the prediction that polar solvents should stabilize this structure even further and therefore facilitate rotation.

To investigate this point, DO3 was studied also for various solvents using the PCM model. In Figure 6 we show the TS

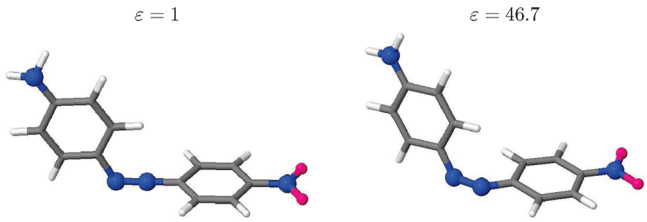

Figure 6. Transition state structures for cis → trans isomerization of DO3 in different "environments".

for cis → trans isomerization of DO3 in the gas phase, which is practically identical to the TS found for nonpolar solvents with small dielectric constants ε, such as heptane. A linear NNC unit is found, indicative of an inversion mechanism. Note that according to Figures 5 (left) and 6 the linearization occurs on the ring, which carries the acceptor. In contrast, a nonlinear transition state is found in polar solvents such as DMSO (ε = 46.7), pointing to a rotational pathway (Figure 5, right).

In Table 6 we show activation energies for DO3 as well as other quantities for a series of solvents studied by PCM. The type of TS (inversion or rotation) is also indicated. From the table, it is noted that in nonpolar solvents the energetics are not much affected as compared to the gas phase. For solvents with $\varepsilon \approx 2$ the classical activation energies are slightly reduced and the reaction is of the inversion type. In contrast, in high ε solvents such as acetone or DMSO, the "zwitterionic" transition state is stabilized: In the acetone PCM field, the energy of the cis form is found to be lowered by 0.70 eV and that of the (new) transition state by 0.89 eV. As a consequence, the classical barrier is reduced by 0.19 eV, relative to the gas phase. The hypothesis that the dipolar resonance structure with a single N−N bond of Figure 4 gains importance is also supported by the computed bond distances: In acetone, we find $r_{NN}^{\ddagger} = 1.291$ Å, while it is only $r_{NN}^{\ddagger} = 1.228$ Å for the linear transition state found in the gas phase. Note, however, that the bond elongation is far from what a true N−N single bond would require. Similar effects are observed for DMSO (ε = 46.7) and other polar solvents. In summary, the rotation mechanism is favored in very polar solvents.

C. Kinetics. ***1. Monosubstituted Azobenzenes.*** In Table 2 we have indicated, for monosubstituted azobenzenes, kinetic parameters such as the cis → trans isomerization rate $k_{c\to t}$ at room temperature, the Arrhenius prefactors A, and effective activation energy E_a. (Note that $k_{c\to t}$(298.15 K) as given in the tables was directly obtained from the Eyring expression; thus when the Arrhenius fit is used and $k_{c\to t}$ recalculated at T = 298.15 K, the two rates are usually not exactly the same.)

From Table 2 we saw that lower classical barriers translate into larger rates. All rate constants (at room temperature) are higher than that for the reference compound AB. Acceptors, in particular in the para position, accelerate the reaction. The species with the largest isomerization rate is 4-NO_2-AB, with an acceleration factor of more than 3000 relative to AB at room temperature. Since all rates are larger than those of AB, one obtains a V-shaped Hammett plot[40] $\log(k_X/k_H)$ vs σ. Here, k_H is the cis → trans isomerization rate constant of azobenzene and k_X is that of the X-substituted species. σ is the substituent constant, whose values are also tabulated in Table 2 and taken from ref 39. In the Hammett plot, which is shown in Figure 7, substituents with positive σ (3-CN, 4-CN, and 4-NO_2) accelerate the reaction, but also substituents with negative σ (4-OMe, 5-NH_2, and 4-NH_2) do. The latter are much less efficient accelerators than the former, rendering the V-shape asymmetric. V-shaped Hammett plots have been found experimentally for substituted azobenzenes in ref 20. All the Arrhenius prefactors A in Table 2 are in the order of 10^{13} s^{-1}. According to the Eyring equation (7), the prefactor is largely determined by the activation entropy, $\Delta S^{\ddagger}$. From the table we note $\Delta S^{\ddagger}$ is positive, with one exception (4-NO_2-AB). The largest $\Delta S^{\ddagger}$ give the largest prefactors. The largest prefactor is for 4-adamantyl-AB, the lowest one for 4-NO_2-AB. The changes ΔC_V of the heat capacity are small and have only a minor effect on overall rates.

2. Push−Pull Azobenzenes. For DO3, the isomerization rates depend strongly on the solvent. As can be seen from Table 6, in very polar solvents the rates increase by up to 2 orders of magnitude relative to nonpolar solvents. This is due to the lower barrier for isomerization in the polar environment as discussed above. Note that the low barriers have to overcompensate the smaller Arrhenius prefactors A in polar solvents. The A factors for acetone and DMSO are by a factor of 5 smaller than the gas phase value. The smaller prefactors are due to the fact that the activation entropies are negative for DO3 in polar solvents (rotation pathway) and increase in magnitude with ε. In contrast, $\Delta S^{\ddagger}$ is small and positive for isolated DO3 or DO3 in nonpolar solvents (inversion pathway). In that sense the rotational transition state is "more ordered". The trend in computed activation entropies as a function of ε is consistent with experimental data.[17] A more negative $\Delta S^{\ddagger}$ for polar solvents implies a smaller Arrhenius prefactor.

The rate acceleration in polar solvents is consistent with experiment. In ref 17 it was experimentally demonstrated for 4-NO_2−4′-NMe_2−AB and related push−pull azobenzenes that quantitatively $k_{c\to t}$ depends on ε roughly according to

$$\ln k_{c\to t} = a + b\left(\frac{\varepsilon - 1}{\varepsilon + 1}\right) \tag{10}$$

where a is the rate at ε = 1 and b is the slope which will be defined shortly. Equation 10 follows from a model of Kirkwood based on the calculation of free energies of molecular, spherical dipoles embedded in a dielectric continuum.[41] Figure 8 shows that our theoretical data set indeed follows a linear relationship as predicted by eq 10.

According to ref 41 and ref 17 the slope of the curve is

$$b = \frac{1}{4\pi\varepsilon_0}\frac{3}{8k_BT}\left(\frac{\mu_{\ddagger}^{\ 2}}{R_{\ddagger}^{\ 3}} - \frac{\mu_c^{\ 2}}{R_c^{\ 3}}\right)$$

where $\mu_{\ddagger}$ and μ_c are the dipole moments of the molecule in the transition state and for the cis form and $R_{\ddagger}$ and R_c are the molecular radii. A positive slope thus indicates that the dipole moment increases in the transition state. That is indeed the case: The computed cis dipole moments are, for the low-ε solvents between 8.6 and 9 D (depending on solvent), and increase to 16−16.5 D in the transition state. For the high-ε solvents acetone and DMSO, the dipole moment changes from ≈11 D for cis, to above 26 D in the transition state. Quantitatively, when using "typical" dipole values (for the low-ε case) of $\mu_c \approx 9$ D, $\mu_{\ddagger} \approx$ 16 D and reasonable estimates for $R_c \approx R_{\ddagger}$ (≈ 6 Å), the slope according to the above formula is around 7.5, which is similar to what one obtains from Figure 8, namely, $b \approx 6.2$. It should be noted, however, that the dipole change is ε-dependent and that the slope depends sensitively on the chosen dipole moments and also on molecular radii. Closer inspection reveals that the slope of the curve is slightly superlinear, reflecting the larger

TABLE 6: DO3 Classical Activation Energies $\Delta E_{el}^{\ddagger}$, Isomerization Rates $k_{c\to t}$ at Room Temperature, Activation Entropies $\Delta S^{\ddagger}$, Arrhenius Prefactors A, and Arrhenius Activation Energies E_a in Different Solvents, Obtained within the PCM Model[a]

solvent	ε	$\Delta E_{el}^{\ddagger}$	$k_{c\to t}$ (298.15 K)	$\Delta S^{\ddagger}$	A	E_a	type
gas phase	1.000	0.77	5.2	1.15	7.06×10^{12}	0.73	inversion
heptane	1.920	0.72	28.2	1.41	7.20×10^{12}	0.68	inversion
cyclohexane	2.023	0.72	30.9	1.35	6.97×10^{12}	0.72	inversion
carbontetrachloride	2.228	0.72	42.5	1.95	7.33×10^{12}	0.67	inversion
benzene	2.247	0.73	75.9	6.34	1.23×10^{13}	0.67	inversion
ether	4.335	0.68	151.4	0.88	5.85×10^{12}	0.64	rotation
chlorobenzene	5.621	0.65	228.1	−4.84	3.92×10^{12}	0.61	rotation
aniline	6.890	0.64	379.9	−5.95	3.61×10^{12}	0.60	rotation
dichlormethane	8.93	0.61	632.7	−9.40	2.54×10^{12}	0.58	rotation
quinoline	9.03	0.62	584.1	−7.56	3.23×10^{12}	0.58	rotation
dichlorethane	10.36	0.61	888.9	−8.77	2.72×10^{12}	0.57	rotation
acetone	20.7	0.58	1326.1	−14.23	1.60×10^{12}	0.55	rotation
DMSO	46.7	0.55	2321.6	−17.37	1.10×10^{12}	0.52	rotation

[a] Energies are in electronvolts, rates and prefactors in s^{-1}, entropies in J/(K mol).

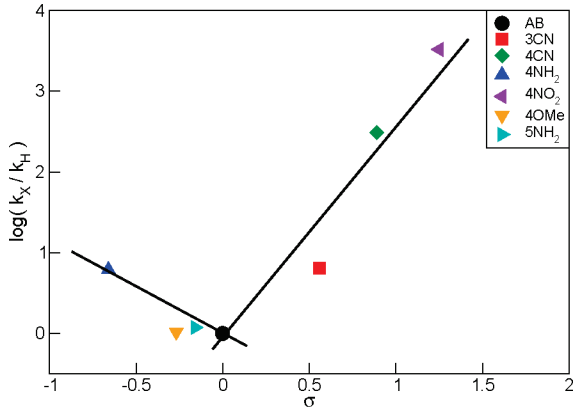

Figure 7. Hammett plot for singly substituted AB molecules. The lines serve as a guide to the eye.

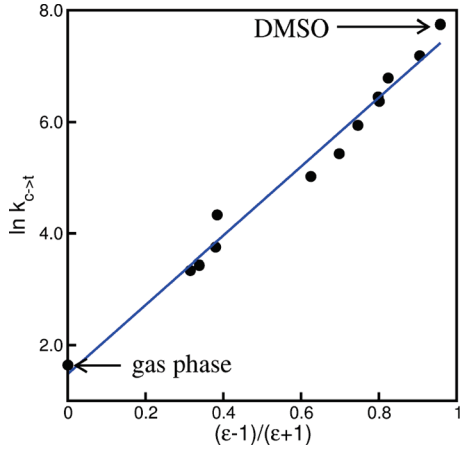

Figure 8. Plot $\ln(k_{c\to t})$ vs $(\varepsilon - 1)/(\varepsilon + 1)$ for DO3 in environments with 13 different "solvents", characterized by different ε, as studied in Table 6. The line is a linear fit to the data.

dipole change in the TS in very polar solvents. However, in a first approximation the Kirkwood model is useful.

3. TBA-based species. To relate to compounds, which have been investigated as molecular switches at surfaces, TBA-based molecules have also been considered. The five molecules TBA, TBA′, DBDCA, diM-TBA, and M-TBA already mentioned in section II are shown in Figure 9 for clarity.

In Table 7, we list results obtained for these species. In all cases the TS was of the inversion type. From the transition states, the rate constants were calculated for $T = 303.15$ K (30 °C). In most examples no PCM field was adopted. For TBA, however, the PCM field of cyclohexane ($\varepsilon = 2.023$) was also considered to estimate the effect of the solvent used in the experiments. The theoretical $\Delta H^{\ddagger}$ values were calculated from $\Delta H^{\ddagger}(T) = \Delta H^{\ddagger}(0) + \Delta C_V^{\ddagger} T$. The experimental $\Delta H^{\ddagger}$ values were determined from a van't Hoff plot $\ln(k/T)$ from rates k, which were determined from time-dependent on UV−vis spectra—see the Supporting Information.

Concerning the theoretical values (left half of the table) for TBA, we observe that similar to the situation found for DO3 (Table 6), cyclohexane slows down the cis → trans isomerization slightly. The solvent effect is only moderate, yet in full agreement with recent findings.[42] The effect of the PCM environment on calculated UV−vis spectra is described in the Supporting Information.

When introducing additional substituents or rearranging *tert*-butyl groups, the following is observed. By adding one donating methoxy group in the para position (M-TBA), the barrier is slightly reduced. However, the rate constant is almost unaltered since simultaneously the Arrhenius prefactor (and the activation entropy) is decreasing relative to TBA. The M-TBA molecule inverts at the ring, which does not carry the −OMe group. A second TS where the inversion occurs on the N-atom adjacent to the ring carrying the −OMe group has a higher activation energy and lower rate. Introducing a second methoxy group at the other ring, also in the para position (diM-TBA) increases the barrier significantly and the rate is decreased by an order of magnitude when compared to TBA. That a single para methoxy group slightly reduces barriers in azobenzenes is in accordance with Table 2, where "ordinary", i.e., nonbulky azobenzenes, were considered. It is also known that two methoxy groups in 4- and 4′-positions lead to larger barriers again. For example, according to Section IIIB the classical barriers $\Delta E_{el}^{\ddagger}$ for AB, 4-OMe-AB, and 4,4′-OMe-AB are 1.17, 1.07, and 1.17 eV, respectively, and hence confirming this result.

The biggest effect in Table 7 is observed after replacement of two *tert*-butyl groups by two carboxyl groups (DBDCA)—in this case the rate increases by a factor of almost 70. Although being attached in meta positions, the two carboxyl groups stabilize the TS via their −I effect in this case. A smaller effect on the rate is found by rearranging the *tert*-butyl groups: The cis → trans rate constant of TBA′ is about 4 times larger than that of TBA, mostly because of an enhanced Arrhenius prefactor. For TBA′, the transition state deviates slightly from linearity ($\alpha = 171°$) most likely due to sterics, which increases $\Delta S^{\ddagger}$ and thus the prefactor.

When comparing theoretical values to experimental data (right half of Table 7), one first of all notes that, perhaps with the

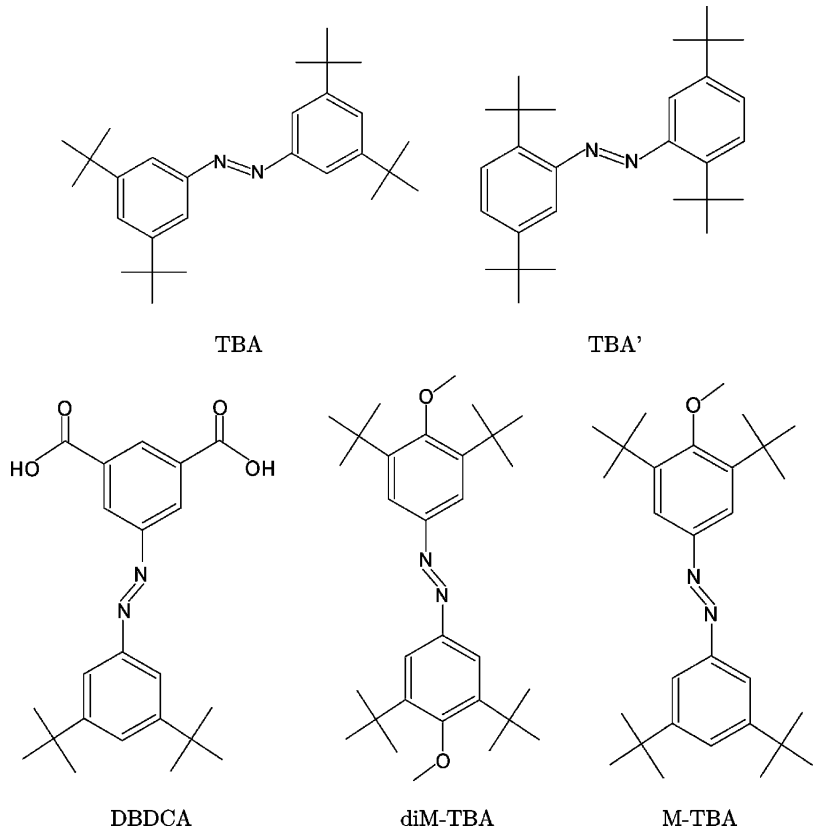

Figure 9. TBA-based azobenzenes studied theoretically and experimentally in this work.

TABLE 7: TBA Derivatives, Rate Parameters, Obtained at $T = 303.15$ K[a]

	theory (gas)			experiment (solvent)		
molecule	$k_{c\to t}$ (303.15 K)	$\Delta S^{\ddagger}$	$\Delta H^{\ddagger}$ (303.15 K)	k_{exp} (303.15 K)	$\Delta S_{exp}{}^{\ddagger}$	$\Delta H_{exp}{}^{\ddagger}$ (303.15 K)
TBA	3.96×10^{-5}	+6.66	1.06			
TBA (cyc-hex)	9.48×10^{-6}	+4.61	1.09	0.35×10^{-6}	-77.0 ± 18.0	0.91 ± 0.06
TBA′	1.40×10^{-4}	+16.22	1.04	4.94×10^{-6}	-50.6 ± 3.7	0.93 ± 0.01
M-TBA	3.18×10^{-5}	+0.84	1.05	0.58×10^{-6}	-37.8 ± 5.2	1.03 ± 0.02
diM-TBA	3.09×10^{-6}	+3.26	1.12	0.85×10^{-6}	-39.0 ± 3.5	1.01 ± 0.01
DBDCA	2.67×10^{-3}	+1.89	0.93	1.18×10^{-6}	-75.8 ± 13.2	0.89 ± 0.04

[a] All measurements were done in cyclohexane, except for DBDCA, where a 10:1 mixture of acetonitrile/MeOH was used. All calculations were done in the gas phase, if not indicated otherwise. TBA = 3,3′,5,5′-tetra-*tert*-butyl-AB; TBA (cyc-hex) = TBA in cyclohexane (also for the calculation); TBA′ = 2,2′,5,5′-tetra-*tert*-butyl-AB; M-TBA = 4-methoxy-3,3′,5,5′-tetra-*tert*-butyl-AB; diM-TBA = 4,4′-dimethoxy−3,3′,5,5′-tetra-*tert*-butyl-AB); DBDCA = 3,5-di-*tert*-butyl−3,5′-dicarboxyl-AB. The energies are in eV, the rates in s^{-1}, the entropies in J/(K mol).

exception of TBA and TBA′, the activation enthalpies $\Delta H^{\ddagger}$ are in good agreement; i.e., experimental and theoretically derived Arrhenius slopes are very similar. There is a big difference, however, regarding the activation entropies $\Delta S^{\ddagger}$, which are small and positive according to theory but large and negative according to experiment. Thus, Arrhenius prefactors are overestimated in theory with the consequence that absolute rates are calculated too small between factors of 3 (for diM-TBA) up to 2000 (for DBDCA). The large deviation for DBDCA is most likely due to the fact that the experiment was carried out in a CH_3CN/MeOH solvent mixture and not in nonpolar cyclohexane, which is well described by the PCM. In this case, hydrogen bonding could also play a decisive role in experiment. Even apart from DBDCA, experimental and theoretical activation entropies are deviating. This remains true when comparing to other experimental sources.[17] Theory thus predicts a "less ordered" TS than experiment. The comparison of results between TBA in the gas phase and TBA in cyclohexane shows that the PCM model does not change the $\Delta S^{\ddagger}$ much. It may well be that, in order to determine such ordering behavior indirectly observed in experiment, the solvent molecules and their thermal motion need to be explicitly included, and a continuum model such as PCM is not sufficient. Further sources of error are the inaccurate calculation of activation entropies in larger molecules when using the harmonic approximation, but also experimental inaccuracies cannot be excluded. Overall theory and experiment agree that the kinetics are not dramatically affected by the substituents under study and that the overall behavior seems similar to the parent nonbulky azobenzenes.

IV. Conclusions and Outlook

An extensive theoretical study has been carried out to address the cis → trans isomerization of substituted azobenzenes in the gas phase and in a polarizable environment. Altogether, around 90 azobenzenes have been studied in this work. For all of them, cis and trans isomers have been calculated and transition states have been searched for. In many cases isomerization rates were

computed. To allow for a systematic theoretical study, as a compromise between computational cost and accuracy the B3LYP/6-31G* model has been chosen, in conjunction with Eyring transition state theory and a PCM to treat solvents.

It was found that in most cases the isomerization reaction proceeds through a linear transition state indicative of an inversion mechanism. The transition state, however, is not reached by pure inversion along the angle α but rather by simultaneous rotation around the CNNC dihedral angle ω. The linear transition state can be stabilized very efficiently with acceptors in ortho and para positions. In the case of double and triple substitution, substituents on one ring have an additive effect on activation energies and kinetics, while for substitution on both rings no simple additivity rule is found. For push−pull azobenzenes the reaction mechanism depends on the solvent, changing from inversion to rotation in polar environments. On a semiquantitative level, the environment increases the rates according to a Kirkwood scenario in which the molecules are treated as dipoles in a polarizable continuum.

Bulky azobenzenes, which were also investigated experimentally in this work, are obtained by adding *tert*-butyl groups. It is found that generally these bulky compounds behave similar to conventional azobenzenes. In this case the kinetics obtained by theory are in good agreement with experimental data, at least as far as activation energies are concerned. Also trends observed by systematic variation of substituents and the polarity of the solvent are nicely reproduced and can be rationalized. For activation entropies and Arrhenius prefactors, however, deviations between theory and experiment are observed. Among the possible reasons for this deviation is the simplified, i.e., nonmicroscopic, treatment of the solvent.

Work to include the solvent at a more detailed, molecular level of theory is currently underway. Another topic of interest is the thermal switching of azobenzenes on a surface, for which interesting differences to solution chemistry have been observed.[8]

Acknowledgment. We thank T. Klamroth (University of Potsdam) for fruitful discussions. We gratefully acknowledge financial support by the Deutsche Forschungsgemeinschaft through the Sonderforschungsbereich 658 (subprojects C2 and B8), and by the Fonds der Chemischen Industrie. S.H. thanks Wacker AG, BASF AG, Bayer Industry Services, and Sasol Germany for generous donations of chemicals.

Supporting Information Available: Descriptions of synthesis of bulky azobenzene derivatives and kinetic analyses of thermal cis → trans isomerization and discussions of the general methods and results for TBA. This material is available free of charge via the Internet at http://pubs.acs.org.

References and Notes

(1) Feringa, B. *Molecular switches*; Wiley-VCH: Weinheim, 2001.
(2) Balzani, V.; Credi, A.; Venturi, M. *Molecular devices and machines. A journey into the nanoworld*; Wiley-VCH: Weinheim, 2003.
(3) Grill, L. *J. Phys: Condens. Matter* **2008**, *20*, 053001.
(4) Alemani, M.; Peters, M.; Hecht, S.; Rieder, K.; Moresco, F.; Grill, L. *J. Am. Chem. Soc.* **2006**, *128*, 14446.
(5) Comstock, M.; Levy, N.; Kirakosian, A.; Cho, J.; Lauterwasser, F.; Harvey, J.; Strubbe, D.; Fréchet, J.; Trauner, D.; Louie, S.; Crommie, M. *Phys. Rev. Lett.* **2007**, *99*, 038301.
(6) Henningsen, N.; Franke, K.; Torrente, I.; Schulze, G.; Priewisch, B.; Rück-Braun, K.; Dokić, J.; Klamroth, T.; Saalfrank, P.; Pascual, J. *J. Phys. Chem. C* **2007**, *111*, 14843.
(7) Tegeder, P.; Hagen, P.; Leyssner, F.; Peters, M.; Hecht, S.; Klamroth, T.; Saalfrank, P.; Wolf, M. *Appl. Phys. A: Mater. Sci. Process.* **2007**, *88*, 465.
(8) Hagen, P.; Kate, P.; Peters, M.; Hecht, S.; Wolf, M.; Tegeder, P. *Appl. Phys. A: Mater. Sci. Process.* **2008**, *93*, 253–260.
(9) Hagen, S.; Leyssner, F.; Nandi, D.; Wolf, M.; Tegeder, P. *Chem. Phys. Lett.* **2007**, *444*, 85.
(10) Wildes, P.; Pacifici, J.; Irick, G., Jr.; Whitten, D. *J. Am. Chem. Soc.* **1971**, *110*, 2004.
(11) Sueyoshi, T.; Nishimura, N.; Yamamoto, S.; Hasegawa, S. *Chem. Lett.* **1974**, *110*, 1131.
(12) Asano, T.; Okada, T. *J. Org. Chem.* **1984**, *49*, 4387.
(13) Hofmann, H.-J.; Cimiraglia, R.; Tomasi, J. *J. Mol. Struct. (THEOCHEM)* **1987**, *152*, 19.
(14) Asano, T.; Furuta, H.; Hofmann, H.-J.; Cimiraglia, R.; Tsuno, Y.; Fujio, M. *J. Org. Chem.* **1993**, *58*, 4418.
(15) Cimiraglia, R.; Asano, T.; Hofmann, H.-J. *Gazz. Chim. Ital.* **1996**, *126*, 679.
(16) Fanghänel, D.; Timpe, G.; Orthmann, V. *Organic Photochromes*; Consultants Bureau: New York, 1990.
(17) Nishimura, N.; Kosako, S.; Sueishi, Y. *Bull. Chem. Soc. Jpn.* **1984**, *57*, 1617.
(18) Kucharski, S.; Janik, R.; Motschmann, H.; Radge, C. *New J. Chem.* **1999**, *23*, 765.
(19) Talaty, E.; Fargo, J. *Chem. Commun.* **1967**, 65.
(20) Nishimura, N.; Sueyoshi, T.; Yamanaka, H.; Imai, E.; Yamamoto, S.; Hasegawa, S. *Bull. Chem. Soc. Jpn.* **1976**, *49*, 1381.
(21) Hammett, L. *Chem. Rev.* **1935**, *17*, 125.
(22) Asano, T.; Yano, T.; Okada, T. *J. Am. Chem. Soc.* **1982**, *104*, 4900.
(23) Becke, A. *J. Chem. Phys.* **1993**, *98*, 5648.
(24) Ditschfield, R.; Hehre, W.; Pople, J. *J. Chem. Phys.* **1971**, *54*, 724.
(25) Hehre, W.; Ditschfield, R.; Pople, J. *J. Chem. Phys.* **1972**, *56*, 2257.
(26) Hariharan, P.; Pople, J. *Theor. Chim. Acta* **1973**, *28*, 213.
(27) Frisch, M.; Trucks, G.; Schlegel, H.; Scuseria, G.; Robb, M.; Cheeseman, J.; Montgomery, Jr., J.; Vreven, T.; Kudin, K.; Burant, J.; Millam, J.; Iyengar, S. S.,and Tomasi, J.; Barone, V.; Mennucci, B.; Cossi, M.; Scalmani, G.; Rega, N.; Petersson, G.; Nakatsuji, H.; Hada, M.; Ehara, M.; Toyota, K.; Fukuda, R.; Hasegawa, J.; Ishida, M.; Nakajima, T.; Honda, Y.; Kitao, O.; Nakai, H.; Klene, M.; Li, X.; Knox, J. E.; Hratchian, H.; Cross, J.; Bakken, V.; Adamo, C.; Jaramillo, J.; Gomperts, R.; Stratmann, R.; Yazyev, O.; Austin, A.; Cammi, R.; Pomelli, C.; Ochterski, J.; Ayala, P.; Morokuma, K.; Voth, G. ; Salvador, P. ; Dannenberg, J.; Zakrzewski, V.; Dapprich, S.; Daniels, A.; Strain, M.; Farkas, O.; Malick, D. K.; Rabuck, A.; Raghavachari, K.; Foresman, J.; Ortiz, J.; Cui, Q.; Baboul, A.; Clifford, S.; Cioslowski, J.; Stefanov, B.; Liu, G.; Liashenko, A.; Piskorz, P.; Komaromi, I.; Martin, R.; Fox, D.; Keith, T.; Al-Laham, M.; Peng, C.; Nanayakkara, A.; Challacombe, M.; Gill, P.; Johnson, B.; Chen, W.; Wong, M.; Gonzalez, C.; Pople, J.; *Gaussian 03*, Revision C.02; Gaussian, Inc: Wallingford, CT, 2004.
(28) Alemani, M.; Peters, M.; Hecht, S.; Rieder, K.; Moresco, F.; Grill, L. *J. Am. Chem. Soc.* **2006**, *128*, 14446.
(29) Alemani, M.; Selvanathan, S.; Ample, F.; Peters, M.; Rieder, K.-H.; Moresco, F.; Joachim, C.; Hecht, S.; Grill, L. *J. Phys. Chem. C* **2008**, *112*, 10509.
(30) Dri, C.; Peters, M.; Schwarz, J.; Hecht, S.; Grill, L. *Nat. Nanotechnol.* **2008**, *3*, 649.
(31) Selvanathan, S.; Peters, M.; Schwarz, J.; Hecht, S.; Grill, L. *Appl. Phys. A: Mater. Sci. Process.* **2008**, *93*, 247.
(32) Peng, C.; Schlegel, H. *Isr. J. Chem* **1993**, *33*, 449.
(33) Peng, C.; Ayala, P.; Schlegel, H.; Frisch, M. *J. Comput. Chem.* **1996**, *17*, 49.
(34) Ayala, P.; Schlegel, H. *J. Chem. Phys.* **1997**, *107*, 375.
(35) H, E. *Chem. Rev* **1935**, *17*, 65.
(36) Mertuš, S.; Scrocco, E.; Tomasi, J. *Chem. Phys.* **1981**, *55*, 117.
(37) Toniolo, A.; Ciminelli, C.; Persico, M.; Martinez, T. *J. Chem. Phys.* **2005**, *123*, 234308–1.
(38) Füchsel, G.; Klamroth, T.; Dokić, J.; Saalfrank, P. *J. Phys. Chem. B* **2006**, *110*, 16337.
(39) Mustroph, H.; Epperlein, J. *J. Prakt. Chem.* **1980**, *322*, 49.
(40) Hammett, L. *Chem. Rev.* **1935**, *17*, 125.
(41) Laidler, K.; Landskroener, P. *Trans. Faraday Soc.* **1956**, *52*, 200.
(42) Briquet, L.; Vercauteren, D.; Perpéte, E.; Jacquemin, D. *Chem. Phys. Lett.* **2006**, *417*, 190.

JP9021344